LANGMUIR Article
Cite This: Langmuir 2017, 33, 12056-12064
pubs.acs.org/Langmuir

Unoccupied Interface and Molecular States in Thiol and Dithiol Monolayers

Jonathan Correa-Puerta,[†,‡] Valeria del Campo,[‡] Ricardo Henríquez,[‡] Vladimir A. Esaulov,[§] Hicham Hamoudi,[∥] Marcos Flores,[⊥] and Patricio Häberle*[,‡]

[†]Instituto de Física, Pontificia Universidad Católica de Valparaíso, 2373223 Valparaíso, Chile
[‡]Departamento de Física, Universidad Técnica Federico Santa María, Av. España 1680, 2390123 Valparaíso, Chile
[§]Institut des Sciences Moléculaires d'Orsay, UMR 8214, CNRS—Université, bât 520, Université Paris-Saclay, Université-Paris Sud, 91405 Orsay, France
[∥]Qatar Environment and Energy Research Institute & Qatar College of Science and Engineering, Hamad Bin Khalifa University, Qatar Foundation, P.O. Box 5825, Doha, Qatar
[⊥]Departamento de Física, FCFM, Universidad de Chile, 8370415 Santiago, Chile

Supporting Information

ABSTRACT: The electronic structure of self-assembled monolayers (SAMs) formed by thiols of different lengths and dithiol molecules bound to Au(111) has been characterized. Inverse photoemission spectroscopy (IPES) and density functional theory have been used to describe the molecule/Au substrate system. All molecular layers display a clear signal in the IPES data at the edge of the lowest unoccupied system orbital (LUSO), roughly 3 eV above the Fermi level. There is also evidence, in both the experimental data and the calculation, of a finite density of states just below the LUSO edge, which has been recognized as localized at the Au-substrate interface. Regardless of the molecular lengths and in addition to this induced density of interface states, an apparent antibonding Au−S state has been identified in the IPES data for both molecular systems. The main difference between the electronic structures of thiol and dithiol SAMs is a shift in the energy of the antibonding state.

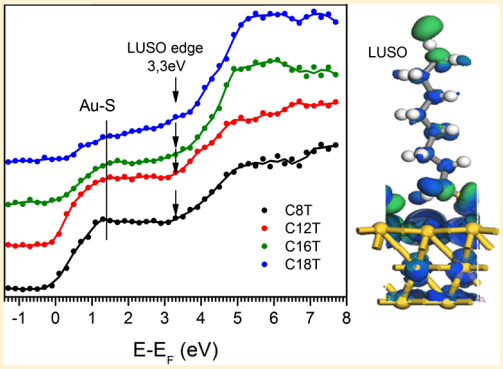

INTRODUCTION

Self-assembled monolayers (SAMs) of organic molecules are considered a very useful component in the formation of nanostructures. They can be instrumental in the modification of the chemical environment of a surface or an electrode, thus affecting the processes of charge transfer, or even assist the formation of nanoscale structures using SAMs as a resist to pattern metallic substrates. These possibilities can be explored because of the particular properties of the molecules that constitute the molecular layer, which under controlled conditions form ordered molecular structures over different substrates. One of the simplest ways to form a SAM is through thiol (R−SH) deposition.[1] The immersion of a metal substrate (noble metal or elements nearby in the periodic table) into a solution of thiols for a few hours induces the formation of a well-ordered molecular layer, with molecules bonded to the substrate by the deprotonated S head group. The simplicity of this method has prompted the development of many research applications, spanning from the surface functionalization to the incorporation of SAMs in devices and detectors.

An interesting property of these molecules is the possibility of modifying the functional end groups, which can modulate the nature of the interaction with the surrounding environment, thus opening new alternatives for basic research and technological applications.[2] For example, the use of thiols as a coating of copper films prevents the formation of oxides at the ambient interface.[3,4] SAMs have also been used as ultrathin organic insulators and incorporated as the dielectric barrier layer in electronic and spintronic devices and also as a gate dielectric in field effect transistors.[5] These types of device-oriented applications require a thorough understanding of the system electronic structure and the different barriers for charge transport along the molecules, including the modifications induced by the coupling of the molecules to the contact electrodes.[6]

For thiols forming a SAM, the orbitals of the anchor group (S) overlap with the electronic states of the substrate, forming what have been defined as system orbitals (SOs). In addition, there is a charge rearrangement at the interface, and new electronic states appear. These new metal-induced states in the case of alkyl chains have been described as an induced density of interface states (IDIS) or metal-induced gap states,[7−9]

Received: August 21, 2017
Revised: October 3, 2017
Published: October 4, 2017

DOI: 10.1021/acs.langmuir.7b02839
Langmuir 2017, 33, 12056−12064

following the nomenclature of semiconductor−metal junctions. Theoretical calculations of the electronic structure of such systems indicate that the influence of the substrate decays rapidly as a function of distance along the alkyl chain. Further away from the substrate, the local density of states (DOS) of the bound molecule is much similar to that of its free counterpart.[10] In practical terms, this hybridization leads to the free-molecule electronic structure, roughly after the first four carbon atoms in the molecular chain away from the substrate.

Detailed information on the electronic structure of the molecules on surfaces, relevant for molecular electronic applications, can be obtained by complementary direct and inverse photoemission measurements. The more commonly utilized ultraviolet photoemission spectroscopy (UPS) provides information on the occupied states, whereas inverse photoemission spectroscopy (IPES) is sensitive to the unoccupied DOS. In IPES, the spectral signal is obtained from a nearly monochromatic electron beam colliding with the surface of interest. The incident electron undergoes, most likely, an optical decay between unoccupied electronic states, and the excess energy is then emitted as a photon. In the so-called isochromat mode, the kinetic energy of the incident electrons is varied and the intensity of photons emitted with a specific energy is detected. In general terms, the IPES intensity can thus be used to map the density of unoccupied states of the monolayer-on-metal system.[11]

A combination of UPS and IPES has been used to study the SAMs of alkyl chains of different lengths adsorbed on silicon substrates.[10,12] The actual energy gap of the monolayers can be determined by examining the intensity of the spectral distribution of emitted photons and electrons. The difference in energy between the onsets of the first more intense features, away from the Fermi level (E_F), in UPS and IPES, can be considered as the optically determined electronic band gap. This interpretation is closely linked to the electronic transport barrier heights, which are mostly defined by the lowest unoccupied and highest occupied alkyl energy levels that extend throughout the complete molecular chain.[10]

Furthermore, the Si/alkyl monolayers display an asymmetry in the location of E_F between the lowest unoccupied SO (LUSO) and the highest occupied SO (HOSO). For alkyl monolayers, E_F is much closer to the prominent features in the unoccupied electronic band. For the case of a metal−molecule SAM of octadecanethiols (C18T) on gold Au(111), Qi et al.[13] obtained an analogous behavior. The UPS and IPES spectra again display tails near E_F and intense features due to HOSO and LUSO states. The IDIS at the metal−molecule interface can be considered relevant in the modulation of the electronic transport across the molecule.

This picture has been made more evident in a recent study of different SAM alkanethiols on gold, characterized using transition voltage spectroscopy (TVS).[14] In TVS, the energy barrier height is directly estimated from current−voltage measurements. Measurements obtained using a conducting atomic force microscopy gold tip[14,15] suggest the presence of interface states. These states display a significant amplitude at a characteristic energy in the range of 1.2−1.3 eV above the E_F of the electrode, thus well-located within the molecular energy gap. In addition, the energy of these resonances seems to be independent of the length of the molecules,[16] as expected for the states located at the molecule−substrate interface.

A closely related SAM system is that formed by dithiol molecules. In these molecules, the two thiol terminations can be used to form a channel between different metallic electrodes.[17−20] Therefore, they have been the subject of intense investigation, mainly because of their potential applications in molecular electronics. The first quantitative electrical measurements on individual molecules were performed in 1,4-benzenedimethanethiols (BDMTs),[21] a molecule that, in addition to the two thiol groups, contains an aromatic ring along the molecular chain. Dithiols can also be used as basic building blocks to form more complex heterostructures,[22,23] in which charge transport should proceed through the channels formed by multimolecular layers. In these applications, the energy of the HOSO and LUSO relative to that of E_F determines the injection barrier height for electrons and holes at the SAM−metal interface. These electronic parameters are central to the device performance[24] of such structures.

Inverse photoemission measurements on alkanethiol SAMs are limited to the C18T case.[12,13] In this paper, we present an extended study for a series of such SAMs ($(CH_2)nSH$, simply defined as CnT, with n = 8, 12, 16, and 18) and also for the prototypical BDMT dithiol case. This investigation complements the earlier direct photoemission measurements on these systems, which provided relevant information on the HOSO edge.[18,25−27] We have used simple numerical calculations of the electronic structure of these systems together with IPES data to describe the origin of relevant optical transitions between unoccupied electronic states of the adsorbed molecules.

EXPERIMENTAL SECTION

The SAMs of octanethiol C8T, dodecanethiol C12T, hexadecanethiol C16T, and octadecanethiol C18T were formed, starting from the liquid phase, and deposited onto a Au(111) single-crystal substrate. The single crystal was prepared in ultrahigh vacuum (UHV) conditions, by repeated cycles of sputtering with 1 keV Ar ions, followed by annealing at 530 °C, prior to the formation of the SAMs. Examination by low-energy electron diffraction and scanning tunneling microscopy (STM) shows that the surface acquires the "herringbone" reconstruction,[28] characteristic of this surface orientation in Au. The crystal was subsequently removed from UHV, and the alkanethiolate SAMs were prepared by dipping the substrate into an alkanethiol−ethanol solution with a concentration of 1 mM at ∼50 °C for 2 h.[19] This procedure is known to produce well-ordered standing up thiol SAMs and has been used by us previously.[19,29,30]

The case of BDMT SAMs is more complex because the outcome of the assembly using, for example, ethanol sometimes yields mixed standing and lying down layers and multilayers. A way of producing reproducibly ordered standing up BDMT SAMs, as checked by infrared spectroscopy and near-edge X-ray absorption fine structure (NEXAFS), has been recently reported by some of us.[8,19,22] For this study, we have used the same procedure to prepare the films. The BDMT SAMs are prepared by immersing the gold crystal into a freshly prepared 1 mM n-hexane solution, for about 30 min at ∼60 °C. The solutions were thoroughly degassed by N_2 bubbling. All of these processes were carried out in the absence of ambient light to avoid photooxidation effects.[18,19] After immersion, the samples were rinsed with a fresh bath of the same solvent, dried out with gaseous N_2, and quickly (<5 min exposure to ambient conditions) inserted back into the characterization chamber, under UHV conditions (base pressure ≈ 2×10^{-10} Torr).

The spectroscopic examination of the unoccupied states was performed with IPES in the isochromat mode. The setup to perform these measurements has been described earlier.[31] Briefly, it consists of an electron source, a variable-energy electron gun (3−20 eV; full width at half-maximum ≈ 0.3 eV), and a photon detector, which is a simple Geiger−Müller counter filled with iodine as a discharge gas and He as a buffer gas. The window that accepts the photons into the Geiger−

DOI: 10.1021/acs.langmuir.7b02839
Langmuir 2017, 33, 12056−12064

Müller tube is a polished SrF_2 disc. The combination of the band gap of the window and the ionization potential of iodine makes this detector highly sensitive to photons in a very narrow band around 9.5 ± 0.2 eV.[32] The angle between the electron gun and the Geiger–Müller detector is ∼45°. The sample is mounted on a goniometer with both an azimuthal rotation and a rotation through an angle theta (θ) around an axis in the plane of the sample. By changing θ, we can change the angle between the surface normal and the incident electrons. All measurements were performed at normal incidence. The binding energies in the collected spectra are referenced to the Fermi edge of the clean Au(111) monocrystal; the data are then displayed as a function of $E-E_F$, with E being the electronic kinetic energy.

The IPES data presented in this paper are averages of spectra recorded at different points on the sample, to improve the statistics while minimizing the exposure of the molecules to the electron beam. The absence of radiation effects was verified by comparing the spectra taken at different times during acquisition. No radiation-induced damage was detected (Figure S1). Several samples were prepared, and IPES measurements were performed under the same conditions with good reproducibility.

STM (Omicron, VT SPM) in UHV (base pressure ≈ 2×10^{-10} Torr) at room temperature conditions was used to characterize the topography of the samples, before and after thiol adsorption. The STM tips were prepared from a Pt/Ir wire (Nanoscience Instruments, 0.25 mm). Their proper operation was determined by verifying atomic resolution on highly oriented pyrolytic graphite before each measurement. The STM images were analyzed using WSxM software.[33]

An X-ray photoelectron spectrometer (PerkinElmer PHI 1257, Al Kα source, 1486.6 eV) was used to examine the chemical environment of the sulfur termination of the BDMT samples.

Numerical Calculations. To gain a better understanding of the different spectral features present in the IPES measurements, a periodic supercell approach in the framework of density functional theory (DFT) was used to calculate the electronic structure of the molecule–gold substrate system. Adsorption energies and DOS were calculated with the CASTEP package.[34] In all simulations, a (2 × 2) unit cell with a vacuum thickness of 30 Å was considered. A plane wave basis set was used to characterize the molecular bonding to the surface. The projected density of states for the molecule–gold interaction was analyzed under the condition of high molecular coverage of the Au(111) surface. The DFT calculations considered ultrasoft pseudopotentials[35] and a 500 eV energy cutoff. The integration over the surface Brillouin zone was done on a 2 × 2 × 1 k-point sampling grid. To reduce the computational time, the gold surface was simulated using a three-layer bulk terminated slab, with static gold atoms. The exchange–correlation interaction has been treated with the generalized gradient approximation as proposed by Perdew–Burke–Ernzerhof.[36]

RESULTS AND DISCUSSION

The characteristics of thiol SAMs are well-known and have been studied by infrared spectroscopy, X-ray photoelectron spectroscopy (XPS), NEXAFS, and STM[18,29,37,38] among other techniques. Although the experimental procedure to reproducibly prepare well-ordered thiol SAMs is known, prior to perform IPES measurements, we did additional tests to ascertain that we do form ordered layers. The characteristics of the thiol molecular arrays were examined by STM and XPS. For the BDMT SAMs, successful STM imaging has never been reported because the possible attachment of the outer SH group to the STM tip may produce significant problems for imaging. We therefore used XPS instead to verify the condition of the surface.

We first outline these results and thereafter discuss the IPES results.

SAM Characterization. Figure 1 shows a collection of representative STM and topographic images of a C8T SAM, collected under UHV conditions and a constant current. The surface is composed of domains with different molecular arrangements. As shown in panels b and c, two kinds of molecular superstructures $c(4\sqrt{3} \times 2\sqrt{3})R30$ and $(\sqrt{3} \times \sqrt{3})R30$[2,39−41] have been identified. In addition to these reconstructions, the topographic image also shows the existence of dark regions, roughly 5 nm in diameter, which correspond to Au "vacancy islands". As previously reported,[42] the SAM is also present in these regions. These vacancies are generated on the crystal during the formation of the molecular layer and have been labeled as "etch pits".[42] The pits shown in Figure 1 are simply holes in the Au substrate, one or two monoatomic layers deep, which are also filled with molecules, in this case with the C8T SAM. This fact becomes evident when the contrast between both regions is modified. Thus, our STM images confirm the formation of ordered thiol SAMs, with the molecules in an upright position.[39,40]

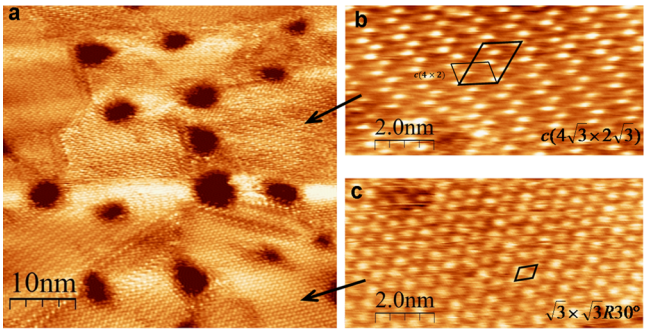

Figure 1. (a) STM image of a C8T SAM formed in an ethanol solution at ∼50 °C (V = −0.55 V and I = 80 pA) and (b,c) high-resolution images taken on each domain of the SAM with c $(4\sqrt{3} \times 2\sqrt{3})$ superstructures and $\sqrt{3} \times \sqrt{3}R30$, respectively ($V$ = −0.6 V and I = 20 pA).

The $\sqrt{3} \times \sqrt{3}R30°$ and $c(4\sqrt{3} \times 2\sqrt{3})$ structures are formed by the adsorption of individual alkanethiolates in different positions of the surface unit cell, such as hollow, bridge, or top sites, of the unreconstructed Au(111) surface.[42] The STM images collected from this surface indicate that the preparation method yields well-ordered molecular monolayers. Similar STM topographic images (not shown here) have also been obtained for the C12T, C16T, and C18T alkanethiolate SAMs, formed using the same preparation procedure.

Considering the fact that it is rather difficult to characterize the BDMT molecules with STM while they are forming the standing up phase,[22] we have used XPS instead to verify the formation of the standing up SAM. As mentioned above, this is an important point in dithiol assembly because there is also the possibility of forming a SAM of lying down molecules with both ends tethered into gold,[22] a feature that is verifiable by using XPS.

The S 2p XPS spectrum shown in Figure 2 corresponds to a typical spectrum of a standing up BDMT SAM. To fit the S 2p peak subcomponents, we have adopted the same procedure as previously described by Hamoudi et al.[19,22] for thiolate SAMs. A Shirley-like background was subtracted from the experimental data; Gaussian functions were used to fit the photoemission peaks. The standard parameters for each S 2p doublet were a 1.2 eV spin–orbit splitting and a 2:1 relation in areas due to the branching ratio between the j = 3/2 and j = 1/2 components. Each doublet is identified in terms of the binding energy of the strongest 3/2 peak. The two principal

DOI: 10.1021/acs.langmuir.7b02839
Langmuir 2017, 33, 12056−12064

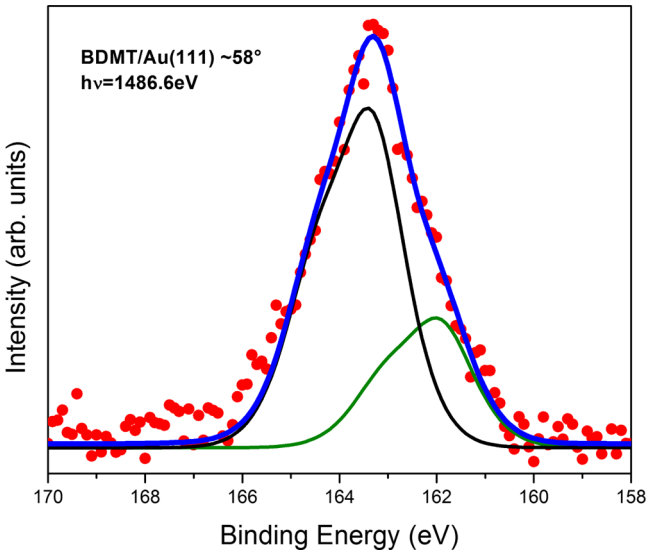

Figure 2. XPS spectrum of the S 2p band collected from a BDMT SAM at a takeoff angle of 58°. The data are fitted using the characteristic double peaks, considering the spin−orbit splitting of the 2p resonance. The thick blue trace (on line) corresponds to the overall fit to the experimental data points. See the text for further details.

doublets are 162 ± 0.2 eV (S_{th}), assigned to the thiolate S−Au bond (green trace in the on-line version of Figure 2), and 163.1 ± 0.2 eV (S_{un}, for unbound) for the SH group at the SAM ambient interface (black trace in the on-line version of Figure 2).

Returning to the main important peaks in the BDMT spectrum, the S_{th}/S_{un} intensity ratio should be suppressed by $\exp(-d/\lambda \sin \theta)$, where d is the layer thickness, λ is the mean free path of electrons in the SAM, and θ is the takeoff angle. Using a value of $\lambda \approx 2.5$ nm,[43] we obtain the values for d in the range of 1.1−1.5 nm. Consistently, the same thickness is obtained from considering the Au 4f attenuation (not shown), as expected for a single layer of BDMT molecules standing in the upright position.[18,19,22]

DFT Calculations. Figure 3 shows the electronic density plots, together with the corresponding ball-bar model of the C8T molecule on Au. The difference between the two plots in a and b is the energy range above E_F, which is being considered. As shown in Figure 3a, for energies between 1 and 2 eV, the p-type orbital of the S anchor group is strongly hybridized with the 5d band in Au, giving rise to antibonding states (unoccupied), mainly localized close to the sulfur group. A different distribution is observed for orbitals between 3 and 5 eV above E_F. Figure 3b shows the projected unoccupied DOS in this energy range. Its amplitude is distributed evenly along the molecule, with higher intensities in σ-type orbitals localized in the carbon and sulfur atoms. In this case, only the higher energy states are expected to play a role in electronic transport along the molecule because the contribution of the low-energy states near E_F is exponentially suppressed compared to that at the LUSO edge, which are spatially distributed, as shown in Figure 3b.

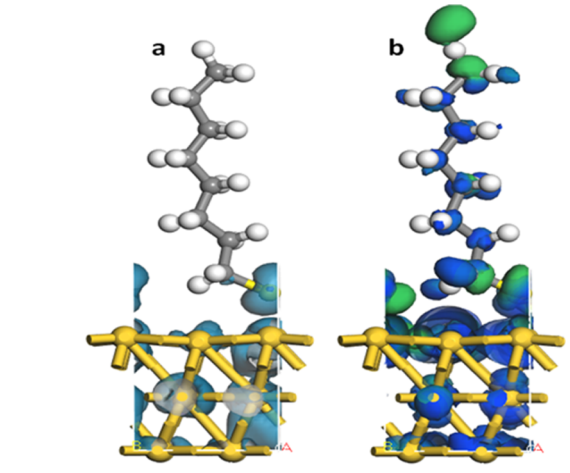

Figure 3. Schematic representation of the spatial distribution of the DOS of C8 molecules adsorbed on Au as obtained from the DFT calculations. Different energy ranges are depicted: (a) between 1 and 2 eV and (b) between 3 and 5 eV above E_F.

IPES from Alkanethiols. The IPES spectra of the unoccupied electronic states of the C8T, C12T, C16T, and C18T SAMs are shown in Figure 4 (vertically displaced for clarity) together with a normal incidence spectrum collected from the Au(111) substrate. The main resonance in this spectrum is a surface state that exists within the projected bulk band gap, close to the Fermi level (~0.5 eV). In addition, at higher energies and close to the vacuum level (~5.3 eV), a less intense feature is detectable, which has been identified as part

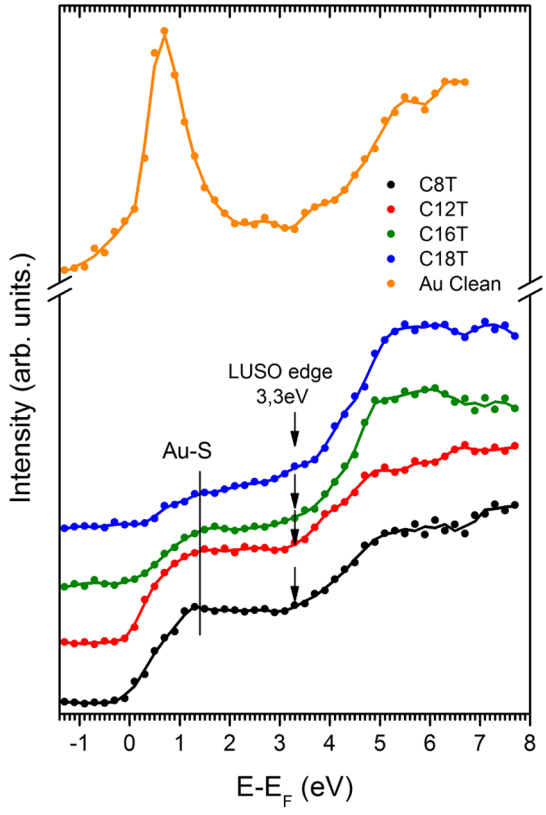

Figure 4. IPES spectra from C8T, C12T, C16T, and C18T alkanethiol SAMs on Au(111), showing the common energy edge of the LUSO for all molecules and the intensity linked to the Au−S antibonding features. The more intense IPES spectra from the clean gold substrate have also been included. The spectra have been displaced vertically for clarity. The vertical line highlights the presence of an interface S−substrate-derived feature, emerging slightly above the rather flat tail intensity. The arrows indicate the LUSO threshold.

DOI: 10.1021/acs.langmuir.7b02839
Langmuir 2017, 33, 12056−12064

of the Rydberg series of image potential states, trapped between the bulk band gap and the vacuum interface.[44]

The C18T spectrum agrees with the general shape reported earlier.[13] All thiol spectra show an onset for the photon intensity close to E_F, a value determined from the measurements performed on the clean Au substrate.

The molecular spectra display some common characteristics: (1) An almost complete suppression of the strong Au substrate signal due mainly to the presence of the molecular layer. (2) There is an initial increase in the photon intensity, which occurs in the first 1 eV above E_F, followed by a flat plateau up to 3 eV. This energy range can be labeled as the "tail" region, in agreement with the previous measurements.[10,12] (3) About 3 eV above E_F, all molecular spectra show a second and more pronounced increase in intensity; this second rise seems to be part of a fairly broad resonance, which extends roughly from 5 to 8 eV. (4) The intensity of the tail plateau relative to that of the second broad resonance scales in inverse proportion to the length of the molecules.

To compare an IPES spectrum, obtained from an array of molecules adsorbed on a substrate, with the corresponding calculation for the partial DOS for the same system, some considerations must be made. This is because the intensity of the photons detected experimentally does not necessarily have a one-to-one correspondence with the amplitude of the DOS of the system for each energy. There are three main aspects to take into account. The first one is the relatively low kinetic energy of the incoming electrons compared to the energy range being sampled in these experiments (≈8 eV). This particular experimental restriction induces a nonnegligible energy dependence of the cross section for optical transitions between the states participating in the generation of the outgoing photons. As a comparison, in a typical UPS experiment performed at a synchrotron facility, the photon excitation energy could be on the order of 100 eV, whereas the energy of the valence band spans only a few electronvolts; in this case, the cross section for optical excitations is fairly constant over the complete energy range of the valence band.

A second relevant point is the actual length of the molecules and the spatial dependence of the DOS. A high DOS feature, located right at the interface, will be slightly suppressed in the measured spectrum, considering the fact that the incident electrons must travel through the electronic density of the SAM before arriving at the interface, hence reducing the effective intensity of the sampling electron beam. This would not be the case if a resonance with a similar binding energy is located right at the free end of the molecules, where no such attenuation exists. As it is evident in our data, this can become a significant effect when the length of the molecules is changed.

Finally, there is the question of the background intensity in IPES. When the energy of the incident electrons is large enough (>10 eV), there are, in general, more nonradiative channels through which partial de-excitations of the incoming electrons can happen. These indirect processes can eventually contribute additional photons competing with direct optical transitions. In general, the latter mechanism induces a steady increase in the background photon intensity in isochromat IPES as a function of incident electron energy. All of these effects combined contribute different weights in the spectral shape; hence, careful considerations are necessary to recognize the DOS features directly from an IPES spectrum.

Figure 5 shows the IPES molecular spectra, together with the numerical calculation of the DOS for the C*n*T−Au system, for

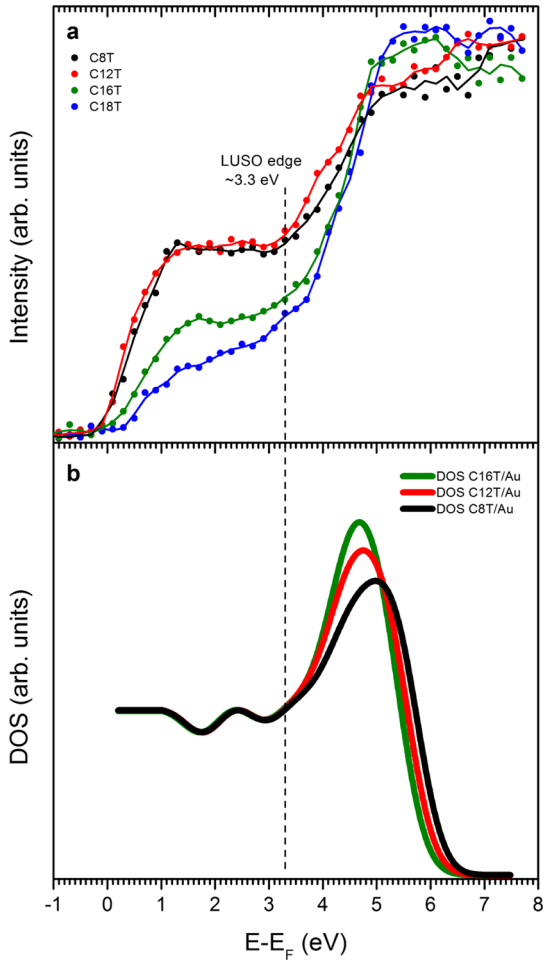

Figure 5. (a) IPES spectra of C8T, C12T, C16T, and C18T alkanethiol SAMs on Au(111) and (b) corresponding theoretical calculation for the DOS of the C*n*T molecules adsorbed on Au. The vertical interrupted line indicates the LUSO edge, common to all SAMs as indicated by both the experimental data and the calculation of the system DOS for selected molecules.

n = 8, 12, and 16. For a suitable comparison between the calculated results and the experimental values, care should be taken to correct the energy of the calculated features to compensate for the limitations in predicting powers of the numerical calculations (the band gap problem).[10,45] The data shown for the unoccupied DOS of C*n*T−Au in Figure 5 have been rigidly shifted by 1.0 eV to align them with the main spectral features in the IPES spectra. This procedure has been done by other authors in the past,[10,45] to allow a proper association of the calculated features with the experimental results.

As free molecules, these C*n*Ts display an energy gap of approximately 7 eV.[46−49] The substrate metal bonding induces the formation of interface states, with a DOS of decreasing magnitude as a function of distance from the substrate along the molecule. A first remarkable aspect made evident by the calculation, as shown in Figure 5, is the nonnegligible value of the DOS for energies between 1 and 2 eV above E_F. It should be kept in mind that for the case of isolated molecules, the DOS intensity in this energy range is close to zero. As shown in Figure 4, the DOS of the SAM in this energy range is mainly derived from the Au−S antibonding orbitals present in all C*n*T molecules, independent of their length.

DOI: 10.1021/acs.langmuir.7b02839
Langmuir 2017, 33, 12056−12064

Roughly 3 eV above E_F, indistinctly for all molecular lengths, the calculations show a sharp increase in the DOS intensity. This sudden rise in the DOS is related to the emergence of s orbitals in the molecular backbone, as shown in Figure 3. This onset can be identified in the calculation as the LUSO edge. The fact that this value turns out to be common for all molecular lengths being considered has also been observed in alkyl molecular chains,[10,16,50−52] either for the molecular band gap or for the lowest unoccupied molecular orbital (LUMO) energy relative to E_F, as it is independent of the number of carbon atoms. Earlier direct photoemission studies[13,25−27] indicate that the HOSO edge for these alkanethiols on Au, as derived from experimental and theoretical calculations, lies about 4.5−5.0 eV below the Fermi level.

It is remarkably evident in the experimental data that there is a clear residual intensity in the low energy range ($E_F < E < 3.3$ eV), which is not directly attributable to Au. This intensity seems to be linked to the so-called IDIS.[12,13] As its name indicates, these are states located precisely at the Au−molecule interface, consistent with the results displayed by our theoretical calculation (Figure 3). A close examination of the relative intensity of the IPES spectra for the different molecules in this energy range ($0 < E < 3.3$ eV), compared to the intensity above the LUSO onset (5.5 eV), indicates that there is a gradual suppression of the IDIS intensity as the length of the molecular chain is increased (see Supporting Figure S2). This length dependence of the ratio between intensities seems to indicate, experimentally, that the states giving rise to these optical transitions are in the tail region and indeed confined to the interface.

Close to E_F, all IPES spectra in Figure 4 show a relatively narrow and weak resonance between 1.2 and 1.4 eV. It is more noticeable for the shorter C8T and C12T molecules and less evident for C16T and C18T, as expected in these cases, because of the stronger mean free path suppression of the incident beam. In agreement with this finding, Nakaya et al.,[53] using scanning tunneling spectroscopy of a C8T SAM on Au(111), found a spectral feature precisely 1.4 eV above E_F. The energy and intensity of this resonance turned out to be rather independent of the local structure of the molecules; either if the C8T was lying down or standing up, it made almost no difference for tunneling into the SAM in this energy range. This result led them to believe that this unoccupied state was derived from a Au−S hybridization, induced by the strong coupling of S to the substrate.[53] This interpretation is somehow confirmed by our data because these states exist for all C*n*T SAMs, considered in this study, precisely in the same energy value, independent of the molecular length.

BDMT: IPES and Calculations. As shown in Figure 6, the IPES response of the BDMT SAM on Au is qualitatively similar to that shown by alkanethiols on the same surface; namely, it has a tail intensity above E_F and a sharp onset close to 3 eV indicating the LUSO edge. Figure 6b displays the shifted DOS (by 2.2 eV) of the unoccupied electronic states, which can be compared directly with the above IPES data. The finite intensity above E_F in the experimental data can be attributed to the IDIS. Within this tail region, the experimental data show a resonance roughly 2.5 eV above E_F. This spectral feature corresponds to the S-derived antibonding state for BDMT−Au, which, in the case of C*n*Ts, as shown above, occurs 1.4 eV above E_F.

Following the criteria established by Segev et al.,[10] we have identified, in the IPES data of Figure 4, the energy of the LUSO

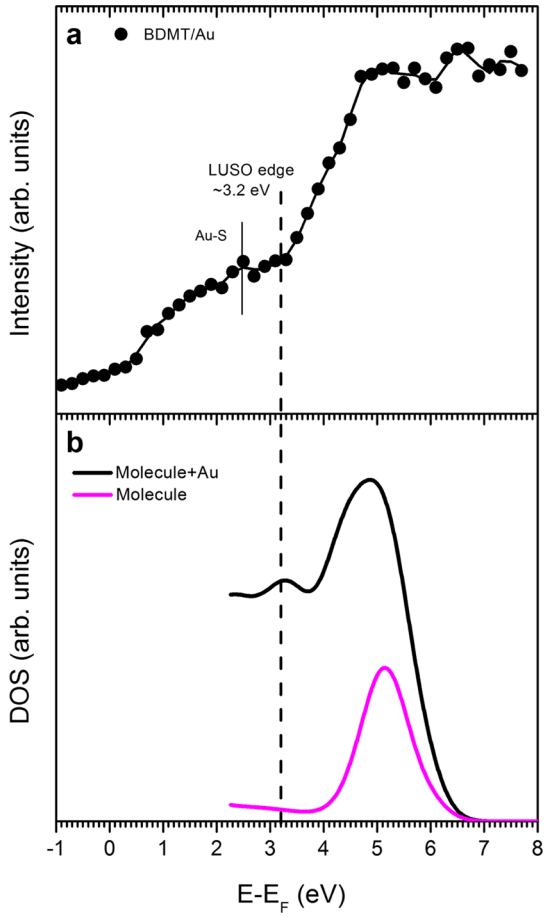

Figure 6. (a) IPES spectra from a BDMT SAM on Au(111). The LUSO edge for this molecule has been identified at 3.2 eV above E_F. (b) DOS of the BDMT−Au system. The black trace corresponds to the total DOS (molecule and Au substrate). The trace in color is just the molecular contribution to the DOS. The difference between both calculated traces is the substrate input to the DOS. The calculations have been displaced to higher energies to align the molecular contribution with the experimental features.

edge as indicated by an arrow in the corresponding spectrum. This assignment is then closely related to the result of the calculation, which shows the same sort of increase in the DOS, precisely at a common value of the energy for the three calculated DOSs. The LUSO energy edge for the C8T, C12T, C16T, and C18T molecules can be identified at 3.2 ± 0.2 eV.

A comparison of the HOSO data from a number of photoemission experiments[25−27] and our LUSO data for the four Au−C*n*T molecular systems (n = 8, 12, 16, and 18) supports the claim by Qi et al.[13] (for C18T) that the Fermi edge is closer to the LUSO energy rather than the HOSO. Our experimental results indicate that this is the case for all C*n*Ts.

The HOSO−LUSO gap and the asymmetry in the location of the Fermi level for BDMT adsorbed on Au can be obtained by examining the occupied DOS. Figure S3 shows the total and partial DOS for the occupied states of the system together with previously reported[18] experimental UPS data. These data indicate that the HOSO edge is roughly 1.6 eV below E_F. To compare with our experimental data, we have also plotted, in Figure 7, the nondisplaced partial DOS. It only includes the molecular contribution to the DOS. The partial DOS linked to the d electron has been excluded, and the s and p partial DOSs are shown separately. The states at the conduction band edge

DOI: 10.1021/acs.langmuir.7b02839
Langmuir 2017, 33, 12056−12064

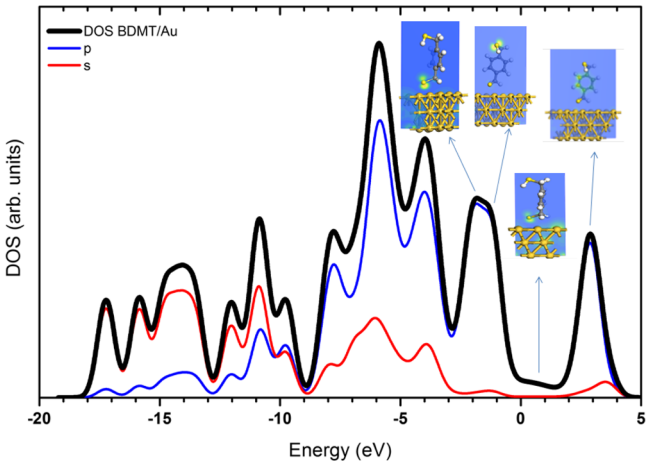

Figure 7. Partial DOS of the molecular contribution to the valence and conduction bands in the BDMT−Au system. The schematic diagrams show the spatial distribution of the DOS at selected energy ranges for both substrate and molecules. To highlight the molecular influence in the electronic structure, only s and p orbitals are considered in the density plot. The contribution of the substrate d electrons has been excluded.

are mainly p orbitals derived from the anchor group (S), which overlap with the interfacial substrate orbitals, forming what has been defined as IDIS. These states are mostly located close to the interface, and as such, they belong to the tail region that penetrates slightly into the molecules from the Au substrate.

The LUSO edge for BDMT is where the second onset, away from E_F occurs, in our spectrum (Figure 6a) 3.2 eV above E_F.The calculation describes correctly the appearance of this feature in the IPES data. As represented in Figure 7, the LUSO comprises mainly the π^* orbital from the aromatic ring of the molecule, in agreement with a previous NEXAFS study of a similar system.[18] As mentioned before, the HOSO edge for the BDMT−Au system is close to 1.6 eV[18,54,55] below E_F (Figure S3). The HOSO edge is thus closer to E_F than the LUSO band. This is indeed opposite to what we have observed for the alkanethiol SAMs on Au, and as suggested earlier, this result may indicate that charge transport across the BDMT SAM is dominated by holes.[45]

CONCLUSIONS

The unoccupied electronic states of SAMs of alkanethiol molecules (C*n*T; n = 8, 12, 16, and 18) and BDMT bound to Au(111) have been described. The IPES spectra for all molecules have many elements in common. There is a strong suppression of the substrate contribution in the spectra measured from the different molecules, in particular the very intense Au surface state, which shows no residual intensity in any of the molecular spectra. Even though the spectra could have contributions from the substrate bulk in the complete energy range being examined, they seem to be minimal, in agreement with the fact that IPES is a quite surface-sensitive technique. Hence, the resulting intensities are dominated by the interface and the molecular contributions. Two onsets in the IPES intensity are recognized in the experimental spectra, one very close to E_F and a second close to 3 eV above E_F for all molecules. As shown in the previous measurements and confirmed by our calculations, there is a new DOS in this energy range, located mostly at the interface (IDIS). The spectral intensity shown by the experimental data seems to have contributions from this particular DOS for all molecules. The second abrupt change in the intensity, close to 3 eV for all molecules, has been identified as the LUSO edge, which correlates with the molecular LUMO, modified by the presence of the Au substrate.

With the aid of theoretical calculations, we were able to perform a qualitative assignment of the symmetry of the different spectral features and recognize their predominance in different spatial locations. IPES also provides relevant information regarding the existence of a Au−S antibonding state, roughly 1.4 eV above E_F for C*n*Ts, quite independent of the molecular length as expected for an interface feature and about 2.5 eV above E_F for BDMT. Both the IDIS and the antibonding states are attenuated for the longer chain molecules. This is an expected behavior because the intensity of the electrons sensing these states is reduced. The probing electrons have to travel through the molecular layer before undergoing the optical transition between states spatially located at the interface.

According to our measurements, in the case of BDMT−Au, the HOSO−LUSO gap is approximately 4.8 eV, with the HOSO edge lying closer to E_F (−1.6 eV) than the LUSO onset (+3.2 eV). For alkanethiol SAMs on Au, the opposite situation occurs. This asymmetry does have some consequences at the moment of considering the sign of charge carriers for the transport along the molecules,[13] in the case of the electrodes are made out of gold.

The results presented here complement previous reports for C*n*Ts and provide new data for the case of BDMT on Au.

ASSOCIATED CONTENT

Supporting Information

The Supporting Information is available free of charge on the ACS Publications website at DOI: 10.1021/acs.langmuir.7b02839.

Sequence of IPES spectra from CT12/Au and CT18/Au, ratio of the intensities below and above the LUSO onset, and total and partial DOS for BDMT-Au (PDF)

AUTHOR INFORMATION

Corresponding Author

*E-mail: patricio.haberle@usm.cl.

ORCID

Vladimir A. Esaulov: 0000-0002-7263-9685

Patricio Häberle: 0000-0003-0840-511X

Author Contributions

The manuscript was written through the contributions of all authors.

Notes

The authors declare no competing financial interest.

ACKNOWLEDGMENTS

This research was partially supported by FONDECYT (grant nos. 1141257, 11140787, and 11121513), CONICYT/CENAVA (grant no. 791100037), and ECOS/CONICYT (grant no. C12E02). J.C.-P. acknowledges MECESUP (grant no. FSM1204) and Doctoral Scholarship from CONICYT 63100001. V.A.E. acknowledges the hospitality of UTFSM, through CONICYT grant MEC 80150073.

DOI: 10.1021/acs.langmuir.7b02839
Langmuir 2017, 33, 12056−12064

REFERENCES

(1) Maksymovych, P.; Voznyy, O.; Dougherty, D. B.; Sorescu, D. C.; Yates, J. T. Gold Adatom as a Key Structural Component in Self-Assembled Monolayers of Organosulfur Molecules on Au(111). *Prog. Surf. Sci.* **2010**, *85*, 206−240.

(2) Schreiber, F. Structure and Growth of Self-Assembling Monolayers. *Prog. Surf. Sci.* **2000**, *65*, 151−257.

(3) Maestre Caro, A.; Travaly, Y.; Beyer, G.; Tokei, Z.; Maes, G.; Borghs, G.; Armini, S. Selective Self-Assembled Monolayer Coating to Enable Cu-to-Cu Connection in Dual Damascene Vias. *Microelectron. Eng.* **2013**, *106*, 76−80.

(4) Ganesan, P. G.; Kumar, A.; Ramanath, G. Surface Oxide Reduction and Bilayer Molecular Assembly of a Thiol-Terminated Organosilane on Cu. *Appl. Phys. Lett.* **2005**, *87*, 011905.

(5) Kong, L.; Chesneau, F.; Zhang, Z.; Staier, F.; Terfort, A.; Dowben, P. A.; Zharnikov, M. Electronic Structure of Aromatic Monomolecular Films: The Effect of Molecular Spacers and Interfacial Dipoles. *J. Phys. Chem. C* **2011**, *115*, 22422−22428.

(6) Zangmeister, C. D.; Robey, S. W.; van Zee, R. D.; Yao, Y.; Tour, J. M. Fermi Level Alignment and Electronic Levels in "Molecular Wire" Self-Assembled Monolayers on Au. *J. Phys. Chem. B* **2004**, *108*, 16187−16193.

(7) Tersoff, J. Schottky Barrier Heights and the Continuum of Gap States. *Phys. Rev. Lett.* **1984**, *52*, 465−468.

(8) Vázquez, H.; Oszwaldowski, R.; Pou, P.; Ortega, J.; Pérez, R.; Flores, F.; Kahn, A. Dipole Formation at metal/PTCDA Interfaces: Role of the Charge Neutrality Level. *Europhys. Lett.* **2004**, *65*, 802−808.

(9) Vázquez, H.; Gao, W.; Flores, F.; Kahn, A. Energy Level Alignment at Organic Heterojunctions: Role of the Charge Neutrality Level. *Phys. Rev. B: Condens. Matter Mater. Phys.* **2005**, *71*, No. 041306(R).

(10) Segev, L.; Salomon, A.; Natan, A.; Cahen, D.; Kronik, L.; Amy, F.; Chan, C. K.; Kahn, A. Electronic Structure of Si(111)-Bound Alkyl Monolayers: Theory and Experiment. *Phys. Rev. B: Condens. Matter Mater. Phys.* **2006**, *74*, 165323.

(11) Watkins, N. J.; Zangmeister, C. D.; Chan, C. K.; Zhao, W.; Ciszek, J. W.; Tour, J. M.; Kahn, A.; van Zee, R. D. Electron Spectra of a Self-Assembled Monolayer on Gold: Inverse Photoemission and Two-Photon Photoemission Spectroscopy. *Chem. Phys. Lett.* **2007**, *446*, 359−364.

(12) Yaffe, O.; Qi, Y.; Scheres, L.; Puniredd, S. R.; Segev, L.; Ely, T.; Haick, H.; Zuilhof, H.; Vilan, A.; Kronik, L.; et al. Charge Transport across Metal/molecular (Alkyl) Monolayer-Si Junctions Is Dominated by the LUMO Level. *Phys. Rev. B: Condens. Matter Mater. Phys.* **2012**, *85*, 045433.

(13) Qi, Y.; Yaffe, O.; Tirosh, E.; Vilan, A.; Cahen, D.; Kahn, A. Filled and Empty States of Alkanethiol Monolayer on Au (111): Fermi Level Asymmetry and Implications for Electron Transport. *Chem. Phys. Lett.* **2011**, *511*, 344−347.

(14) Ricœur, G.; Lenfant, S.; Guérin, D.; Vuillaume, D. Molecule/electrode Interface Energetics in Molecular Junction: A "transition Voltage Spectroscopy" study. *J. Phys. Chem. C* **2012**, *116*, 20722−20730.

(15) Nose, D.; Dote, K.; Sato, T.; Yamamoto, M.; Ishii, H.; Noguchi, Y. Effects of Interface Electronic Structures on Transition Voltage Spectroscopy of Alkanethiol Molecular Junctions. *J. Phys. Chem. C* **2015**, *119*, 12765−12771.

(16) Beebe, J. M.; Kim, B.; Frisbie, C. D.; Kushmerick, J. G. Measuring Relative Barrier Heights in Molecular Electronic Junctions with Transition Voltage Spectroscopy. *ACS Nano* **2008**, *2*, 827−832.

(17) Horiguchi, K.; Tsutsui, M.; Kurokawa, S.; Sakai, A. Electron Transmission Characteristics of Au/1,4-benzenedithiol/Au Junctions. *Nanotechnology* **2009**, *20*, 025204.

(18) Pasquali, L.; Terzi, F.; Seeber, R.; Nannarone, S.; Datta, D.; Dablemont, C.; Hamoudi, H.; Canepa, M.; Esaulov, V. A. UPS, XPS, and NEXAFS Study of Self-Assembly of Standing 1,4-Benzenedimethanethiol SAMs on Gold. *Langmuir* **2011**, *27*, 4713−4720.

(19) Hamoudi, H.; Prato, M.; Dablemont, C.; Cavalleri, O.; Canepa, M.; Esaulov, V. A. Self-Assembly of 1,4-Benzenedimethanethiol Self-Assembled Monolayers on Gold. *Langmuir* **2010**, *26*, 7242−7247.

(20) Hamoudi, H. Crossbar Nanoarchitectonics of the Crosslinked Self-Assembled Monolayer. *Nanoscale Res. Lett.* **2014**, *9*, 287.

(21) Andres, R. P.; Bein, T.; Dorogi, M.; Feng, S.; Henderson, J. I.; Kubiak, C. P.; Mahoney, W.; Osifchin, R. G.; Reifenberger, R. "Coulomb Staircase" at Room Temperature in a Self-Assembled Molecular Nanostructure. *Science* **1996**, *272*, 1323−1325.

(22) Hamoudi, H.; Esaulov, V. A. Selfassembly of α,ω-Dithiols on Surfaces and Metal Dithiol Heterostructures. *Ann. Phys.* **2016**, *528*, 242−263.

(23) Hamoudi, H.; Uosaki, K.; Ariga, K.; Esaulov, V. A. Going beyond the Self-Assembled Monolayer: Metal Intercalated Dithiol Multilayers and Their Conductance. *RSC Adv.* **2014**, *4*, 39657−39666.

(24) Velev, J.; Dowben, P.; Tsymbal, E.; Jenkins, S.; Caruso, A. Interface Effects in Spin-Polarized Metal/insulator Layered Structures. *Surf. Sci. Rep.* **2008**, *63*, 400−425.

(25) Alloway, D. M.; Hofmann, M.; Smith, D. L.; Gruhn, N. E.; Graham, A. L.; Colorado, R.; Wysocki, V. H.; Lee, T. R.; Lee, P. A.; Armstrong, N. R. Interface Dipoles Arising from Self-Assembled Monolayers on Gold: UV−Photoemission Studies of Alkanethiols and Partially Fluorinated Alkanethiols. *J. Phys. Chem. B* **2003**, *107*, 11690−11699.

(26) Duwez, A.-S.; Ghijsen, J.; Riga, J.; Deleuze, M.; Delhalle, J. Surface Molecular Structure of Self-Assembled Alkanethiols Evidenced by UPS and Photoemission with Synchrotron Radiation. *J. Phys. Chem. B* **1997**, *101*, 884−890.

(27) Jia, J.; Mukherjee, S.; Hamoudi, H.; Nannarone, S.; Pasquali, L.; Esaulov, V. A. Lying-Down to Standing-Up Transitions in Self Assembly of Butanedithiol Monolayers on Gold and Substitutional Assembly by Octanethiols. *J. Phys. Chem. C* **2013**, *117*, 4625−4631.

(28) Barth, J. V.; Brune, H.; Ertl, G.; Behm, R. J. Scanning Tunneling Microscopy Observations on the Reconstructed Au(111) Surface: Atomic Structure, Long-Range Superstructure, Rotational Domains, and Surface Defects. *Phys. Rev. B: Condens. Matter Mater. Phys.* **1990**, *42*, 9307−9318.

(29) Vericat, C.; Vela, M. E.; Benitez, G. A.; Gago, J. A. M.; Torrelles, X.; Salvarezza, R. C. Surface Characterization of Sulfur and Alkanethiol Self-Assembled Monolayers on Au(111). *J. Phys.: Condens. Matter* **2006**, *18*, R867−R900.

(30) Pi, U. H.; Kim, J. H.; Yu, H. Y.; Park, C. W.; Choi, S.-Y.; Kim, Y.-K.; Ha, J. S. Enhanced Surface Evolution Induced by the Molecular Desorption in Dodecanethiol Self-Assembled Monolayer on Au(111). *Surf. Sci.* **2006**, *600*, 625−631.

(31) Denninger, G.; Dose, V.; Scheidt, H. A VUV Isochromat Spectrometer for Surface Analysis. *Appl. Phys.* **1979**, *18*, 375−380.

(32) Häberle, P.; Ibañez, W.; Esparza, R.; Vargas, P. Unoccupied Electronic States of Au(113): Theory and Experiment. *Phys. Rev. B: Condens. Matter Mater. Phys.* **2001**, *63*, 235412.

(33) Horcas, I.; Fernández, R.; Gómez-Rodríguez, J. M.; Colchero, J.; Gómez-Herrero, J.; Baro, A. M. WSXM: A Software for Scanning Probe Microscopy and a Tool for Nanotechnology. *Rev. Sci. Instrum.* **2007**, *78*, 013705.

(34) Clark, S. J.; Segall, M. D.; Pickard, C. J.; Hasnip, P. J.; Probert, M. I. J.; Refson, K.; Payne, M. C. First Principles Methods Using CASTEP. *Z. Kristallogr.* **2005**, *220*, 567−570.

(35) Becke, A. D. Density-Functional Exchange-Energy Approximation with Correct Asymptotic Behavior. *Phys. Rev. A* **1988**, *38*, 3098−3100.

(36) Perdew, J. P.; Burke, K.; Ernzerhof, M. Generalized Gradient Approximation Made Simple. *Phys. Rev. Lett.* **1996**, *77*, 3865−3868.

(37) Love, J. C.; Estroff, L. A.; Kriebel, J. K.; Nuzzo, R. G.; Whitesides, G. M. Self-Assembled Monolayers of Thiolates on Metals as a Form of Nanotechnology. *Chem. Rev.* **2005**, *105*, 1103−1170.

(38) Laiho, T.; Leiro, J. A.; Lukkari, J. XPS Study of Irradiation Damage and Different Metal-Sulfur Bonds in Dodecanethiol Monolayers on Gold and Platinum Surfaces. *Appl. Surf. Sci.* **2003**, *212−213*, 525−529.

DOI: 10.1021/acs.langmuir.7b02839
Langmuir 2017, 33, 12056−12064

(39) Poirier, G. E. Characterization of Organosulfur Molecular Monolayers on Au(111) Using Scanning Tunneling Microscopy. *Chem. Rev.* **1997**, *97*, 1117−1128.
(40) Pi, U. H.; Jeong, M. S.; Kim, J. H.; Yu, H. Y.; Park, C. W.; Lee, H.; Choi, S.-Y. Current Flow through Different Phases of Dodecanethiol Self-Assembled Monolayer. *Surf. Sci.* **2005**, *583*, 88−93.
(41) Correa-Puerta, J.; Del Campo, V.; Henríquez, R.; Häberle, P. Resistivity of Thiol-Modified Gold Thin Films. *Thin Solid Films* **2014**, *570*, 150−154.
(42) Vericat, C.; Vela, M. E.; Benitez, G.; Carro, P.; Salvarezza, R. C. Self-Assembled Monolayers of Thiols and Dithiols on Gold: New Challenges for a Well-Known System. *Chem. Soc. Rev.* **2010**, *39*, 1805−1834.
(43) Lamont, C. L. A.; Wilkes, J. Attenuation Length of Electrons in Self-Assembled Monolayers of n-Alkanethiols on Gold. *Langmuir* **1999**, *15*, 2037−2042.
(44) Woodruff, D. P.; Royer, W. A.; Smith, N. V. Empty Surface States, Image States, and Band Edge on Au(111). *Phys. Rev. B: Condens. Matter Mater. Phys.* **1986**, *34*, 764−767.
(45) Feng, D.-Q.; Wisbey, D.; Losovyj, Y. B.; Tai, Y.; Zharnikov, M.; Dowben, P. A. Electronic Structure and Polymerization of a Self-Assembled Monolayer with Multiple Arene Rings. *Phys. Rev. B: Condens. Matter Mater. Phys.* **2006**, *74*, 165425.
(46) Muntwiler, M.; Lindstrom, C. D.; Zhu, X.-Y. Delocalized Electron Resonance at the Alkanethiolate Self-Assembled monolayer/Au (111) interface. *J. Chem. Phys.* **2006**, *124*, 081104.
(47) Salomon, A.; Cahen, D.; Lindsay, S.; Tomfohr, J.; Engelkes, V. B.; Frisbie, C. D. Comparison of Electronic Transport Measurements on Organic Molecules. *Adv. Mater.* **2003**, *15*, 1881−1890.
(48) Tomfohr, J.; Sankey, O. F. Complex Band Structure, Decay Lengths, and Fermi Level Alignment in Simple Molecular Electronic Systems. *Phys. Rev. B: Condens. Matter Mater. Phys.* **2002**, *65*, 245105.
(49) Yaffe, O.; Scheres, L.; Segev, L.; Biller, A.; Ron, I.; Salomon, E.; Giesbers, M.; Kahn, A.; Kronik, L.; Zuilhof, H.; et al. Hg/Molecular Monolayer−Si Junctions: Electrical Interplay between Monolayer Properties and Semiconductor Doping Density. *J. Phys. Chem. C* **2010**, *114*, 10270−10279.
(50) Song, H.; Kim, Y.; Jeong, H.; Reed, M. A.; Lee, T. Coherent Tunneling Transport in Molecular Junctions. *J. Phys. Chem. C* **2010**, *114*, 20431−20435.
(51) Vuillaume, D.; Boulas, C.; Collet, J.; Allan, G.; Delerue, C. Electronic Structure of a Heterostructure of an Alkylsiloxane Self-Assembled Monolayer on Silicon. *Phys. Rev. B: Condens. Matter Mater. Phys.* **1998**, *58*, 16491−16498.
(52) Mirjani, F.; Thijssen, J. M.; van der Molen, S. J. Advantages and Limitations of Transition Voltage Spectroscopy: A Theoretical Analysis. *Phys. Rev. B: Condens. Matter Mater. Phys.* **2011**, *84*, 115402.
(53) Nakaya, M.; Shikishima, M.; Shibuta, M.; Hirata, N.; Eguchi, T.; Nakajima, A. Molecular-Scale and Wide-Energy-Range Tunneling Spectroscopy on Self-Assembled Monolayers of Alkanethiol Molecules. *ACS Nano* **2012**, *6*, 8728−8734.
(54) Pasquali, L.; Terzi, F.; Seeber, R.; Doyle, B. P.; Nannarone, S. Adsorption Geometry Variation of 1,4-Benzenedimethanethiol Self-Assembled Monolayers on Au(111) Grown from the Vapor Phase. *J. Chem. Phys.* **2008**, *128*, 134711.
(55) Pasquali, L.; Mukherjee, S.; Terzi, F.; Giglia, A.; Mahne, N.; Koshmak, K.; Esaulov, V.; Toccafondi, C.; Canepa, M.; Nannarone, S. Structural and Electronic Properties of Anisotropic Ultrathin Organic Films from Dichroic Resonant Soft X-Ray Reflectivity. *Phys. Rev. B: Condens. Matter Mater. Phys.* **2014**, *89*, 045401.

DOI: 10.1021/acs.langmuir.7b02839
Langmuir 2017, 33, 12056−12064